Journal of Bioscience and Bioengineering
VOL. 128 No. 3, 355–364, 2019

www.elsevier.com/locate/jbiosc

Magnetically triggered transgene expression in mammalian cells by localized cellular heating of magnetic nanoparticles

Akira Ito,[1] Ryoji Teranishi,[1] Kazuki Kamei,[1] Masaki Yamaguchi,[1] Akihiko Ono,[2] Shinya Masumoto,[1] Yuto Sonoda,[1] Masanobu Horie,[3] Yoshinori Kawabe,[1] and Masamichi Kamihira[1,2,*]

Department of Chemical Engineering, Faculty of Engineering, Kyushu University, 744 Motooka, Nishi-ku, Fukuoka 819-0395, Japan,[1] Graduate School of Systems Life Sciences, Kyushu University, 744 Motooka, Nishi-ku, Fukuoka 819-0395, Japan,[2] and Division of Biochemical Engineering, Radioisotope Research Center, Kyoto University, Yoshida Konoe-cho, Sakyo-ku, Kyoto 606-8501, Japan[3]

Received 14 January 2019; accepted 11 March 2019
Available online 5 April 2019

To develop a remote control system of transgene expression through localized cellular heating of magnetic nanoparticles, a heat-inducible transgene expression system was introduced into mammalian cells. Cells were labeled with magnetic nanoparticles and exposed to an alternating magnetic field. The magnetically labeled cells expressed the transgene in a monolayer and multilayered cell sheets in which cells were heated around the magnetic nanoparticles without an apparent temperature increase in the culture medium. Magnetic cells were also generated by genetically engineering with a ferritin gene, and transgene expression could be induced by exposure to an alternating magnetic field. This approach may be applicable to the development of novel gene therapies in cell-based medicine.

[**Key words:** Magnetic nanoparticle; Synthetic biology; Tissue engineering; Heat shock protein promoter; Ferritin]

Synthetic biology, which aims to standardize and expand the natural tool box of biological building blocks to engineer novel synthetic networks in a living system (1), has significantly advanced the design of synthetic gene expression systems in designer cells that provide new treatment strategies for a variety of medical conditions (2). As a biological building block in the bioengineer's tool box, promoters can be fundamental gene switches. Expression of human heat shock protein 70B' (HSP70B') is upregulated by heat stress through binding of heat shock factors to the heat shock element (3). The HSP70B' promoter has been used as a heat inducible promoter with very low basal expression levels (4). Synthetic transcription factors, including tetracycline (Tet)-controlled expression systems, can also be ideal building blocks to construct synthetic gene expression systems (5). In the Tet-transactivator system, the *Escherichia coli*-derived Tet-repressor is fused with the herpes simplex-1 viral transcriptional activator VP16 to create a Tet-responsive transcriptional activator (tTA). The DNA-binding domain of tTA recognizes a Tet-responsive element (TRE) sequence as a cognate DNA sequence, which is linked to a proximal minimal CMV promoter region ($P_{CMVmini}$) located upstream of a gene of interest. Thus, tTA induces transgene expression at a high level through binding to the TRE region, and the addition of Tet or its analog, doxycycline (Dox), varies the interaction between tTA and TRE, leading to regulation of transgene expression. By combining these building blocks, we previously developed a heat-inducible transgene expression system with tightly heat-inducible and high level expression (6), in which the heat-activated HSP70B' promoter drives bicistronic gene expression of a target transgene and tTA gene, which is mediated by an internal ribosomal entry site (IRES). Then, the tTA protein binds and activates TRE/$P_{CMVmini}$ upstream of the target transgene, which in turn induces further expression of the target transgene and tTA genes, providing a transcriptional positive feedback loop.

Magnetic heating of nanoparticles has been an active area in nanotechnology, and magnetic fluid hyperthermia (MFH) is a typical biomedical application (7–9). Technically, MFH consists of injecting magnetic nanoparticles directly into tumor tissue, and then damaging the tumor selectively by applying an alternating magnetic field (AMF) from outside of the body to induce heat generation within the nanoparticles via hysteresis loss and/or relaxational loss (10,11). Typically, nanoparticles made of magnetite (Fe_3O_4) or maghemite (Fe_2O_3) have been used. For the heating apparatus, magnetic fields with the order of tens of kA/m at several 100 kHz are generated inside of a coil. Previously, to improve targeting of magnetite nanoparticles to tumor cells, magnetite cationic liposomes (MCLs) were developed by encapsulating 10 nm magnetite nanoparticles in cationic liposomes (12). In 2011, Imai et al. (13) started a phase I clinical trial of MFH using MCLs for patients with head and neck, breast, and soft tissue malignant tumors refractory to conventional therapy. In our preclinical study of MFH (14), MCLs and the heat-inducible transgene expression system were introduced into mouse B16 melanoma *in vivo*, and the magnetically triggered tumor necrosis factor-α gene expression resulted in strong tumor growth inhibition. This combination therapy of hyperthermia and gene therapy showed great potential for cancer treatment.

* Corresponding author at: Department of Chemical Engineering, Faculty of Engineering, Kyushu University, 744 Motooka, Nishi-ku, Fukuoka 819-0395, Japan. Tel.: +81 92 802 2743; fax: +81 92 802 2793.
E-mail address: kamihira@chem-eng.kyushu-u.ac.jp (M. Kamihira).

1389-1723/$ – see front matter
https://doi.org/10.1016/j.jbiosc.2019.03.008

A remote activation system of target cells to trigger specific gene expression can provide a useful biological research tool and may be a novel approach for controlled expression of therapeutic genes in cell-based medicine including regenerative medicine. Compared with other remote activation systems such as optical stimulation (15), cell activation by a magnetic field is advantageous because a magnetic field can penetrate deep into the body and has almost no interactions with biological molecules. Here, we present an approach employing localized cellular heating of magnetic nanoparticles to convert an external magnetic signal into cellular stimulation. The heat-inducible transgene expression system was introduced into mammalian cells using a retroviral vector. MCLs were targeted to the cells and heated by an AMF. Unlike hyperthermia (>43°C), the cells should not be killed by heating. In the present study, we show that magnetically labeled cells can express a transgene through exposure to an AMF in a monolayer and multilayered cell sheets without bulk heating of culture medium.

The above approaches require application of functionalized magnetite nanoparticles to target cells. An alternative is to genetically synthesize magnetic nanoparticles in target cells using an iron storage protein, ferritin, which forms naturally occurring magnetic iron nanoparticles (16). Ferritin is a spherical protein (12 nm in diameter) consisting of 24 subunits of ferritin heavy and light chains (16). Iordanova et al. (17) reported that transfection of a gene encoding a fusion protein of the ferritin light chain, a flexible linker, and ferritin heavy chain increased the iron-loading ability and enhanced the NMR transverse relaxation rate $R_2 (= 1/T_2)$ of cell pellets, suggesting a promising probe-less magnetic resonance imaging (MRI) reporter. However, there is room to improve the iron content in ferritin-engineered cells. Based on the mechanism of dietary Fe^{2+} iron transport into the intestinal lumen, Kim et al. (18) combined the iron importer divalent metal ion transferase 1 (DMT1) gene with the ferritin gene to enhance cellular iron uptake and iron mineralization in ferritin nanoparticles. However, because Fe^{3+} iron in circulation binds to transferrin, which in turn binds to the transferrin receptor in the plasma membrane followed by endocytosis in a receptor-mediated manner (19), transferrin is an important iron-transport component. In the present study, we investigated these approaches to augment iron uptake by target cells, and found that magnetic cells can be generated by genetically engineering with a ferritin gene, and AMF exposure induced transgene expression in multilayered cell sheets.

MATERIALS AND METHODS

Cell culture Human hepatoblastoma HepG2 cells and human cervical carcinoma HeLa cells were maintained in Dulbecco's modified Eagle's medium (DMEM; high glucose, 4.5 g/L) supplemented with 10% fetal bovine serum (FBS) and antibiotics (0.1 mg/mL streptomycin sulfate and 100 U/mL potassium penicillin G). 293FT cells were used as producers of the retroviral vector based on the Moloney murine leukemia virus and cultured in high glucose DMEM supplemented with 10% FBS, 0.1 mM MEM non-essential amino acids (Invitrogen, Carlsbad, CA, USA), 20 mM 4-(2-hydroxyethyl)piperazine-1-ethanesulfonic acid (HEPES; Dojindo, Kumamoto, Japan), and antibiotics. All cells were cultured on collagen-coated tissue culture dishes (Asahi Techno Glass, Tokyo, Japan) at 37°C in a humidified atmosphere with 5% CO_2.

Retroviral vector production and infection The structure of the retroviral vector used in this study is shown in Fig. S1A. The plasmid pHSP/TRE/EGFP/IRES/tTA (14) was digested with *Kpn*I, *Sca*I, and *Pvu*II. The plasmid pQMSCV/EGFP/TRE/DsRed/WPRE (20) was digested with *Eco*RI and *Cla*I. The DNA fragments were ligated together to generate the retroviral vector plasmid pQMSCV/HSP/TRE/EGFP/IRES/tTA.

Retroviral vectors pseudotyped with the vesicular stomatitis G protein (VSV-G) were produced by transient transfection of 293FT cells with three plasmid DNAs, the retroviral vector plasmid (pQMSCV/HSP/TRE/EGFP/IRES/tTA), pcDNA4-gag/pol (21), and pLP/VSV-G (21), using Lipofectamine 2000 (Invitrogen). Culture medium containing retroviral particles was filtered to remove cell debris using a 0.45-μm cellulose acetate filter (Advantec, Tokyo, Japan). The viral solution was then concentrated by centrifugation (60,000 ×*g* at 4°C for 2 h). After removal of the supernatant, the viral pellet was suspended in 50 mM Tris-HCl buffer (pH 7.8) containing 130 mM NaCl and 1 mM EDTA. The viral titer was determined using a Retrovirus Titer Set (for Real Time PCR) (Takara Bio, Shiga, Japan). For retroviral infection, HepG2 cells (4×10^4/well) were seeded in 24-well tissue culture plates (Greiner Bio-One, Frickenhausen, Germany). After 1 day of culture, the medium was replaced with fresh medium containing concentrated viral solutions (multiplicity of infection: 10) and 8 μg/mL polybrene (Sigma–Aldrich, St. Louis, MO, USA). The cells were incubated at 37°C for 6 h, and then the medium was changed to fresh medium. We established a clone with heat-inducible expression of enhanced green fluorescent protein (EGFP), which was designated as HepG2-HSP.

Water bath heating HepG2-HSP cells (2×10^5) were seeded in 35-mm collagen-coated culture dishes (Asahi Techno Glass). After 24 h of incubation, the dishes were sealed and directly immersed in a calibrated water bath (WB) at 39°C, 41°C, or 43°C for 60 min. After WB heating, the dishes were immediately returned to the 37°C CO_2 incubator. At 48 h after WB heating, HepG2-HSP cells were observed under a fluorescence microscope (BZ-9000; Keyence, Osaka, Japan), and the expression level of EGFP was analyzed by flow cytometry (SH800 Cell Sorter; Sony, Tokyo, Japan). The number of viable cells at 48 h after WB heating was assessed using the trypan blue dye exclusion method, and the percentage of viable cells was determined as follows: cell viability (%) = (the number of viable cells in the tested dish)/(the number of viable cells in the non-heated control dish) × 100. Cell sorting for EGFP-positive cells was performed using the SH800 Cell Sorter. The sorted cells were cultured in medium containing Dox for 1 week to suppress EGFP expression mediated by the Tet-transactivator system. The cells were then cultured in medium without Dox for 3 days and heated again in the WB at 41°C or 43°C for 60 min in the presence or absence of Dox. Dox treatments were performed by culturing the cells in medium containing 1 μg/mL Dox.

Preparation of MCLs The magnetite nanoparticles (Fe_3O_4; average particle size: 10 nm) used as the core of the MCLs were purchased from Toda Kogyo (Hiroshima, Japan). We prepared MCLs using colloidal magnetite and a lipid mixture of *N*-(α-trimethylammonioacetyl)-didodecyl-D-glutamate chloride (TMAG; Sogo Pharmaceutical, Tokyo, Japan), dilauroylphosphatidyl-choline (DLPC; NOF, Tokyo, Japan), and dioleoylphosphatidyl-ethanolamine (DOPE; NOF) at a 1:2:2 molar ratio as described previously (12). Briefly, the lipid mixture dissolved in chloroform was dried by evaporation for a minimum of 30 min. Lipids were hydrated by vortexing in colloidal magnetite nanoparticles, and the liposomes were sonicated for 60 min.

Magnetic heating of monolayered HepG2-HSP cells with MCLs HepG2-HSP cells (2×10^5) were seeded in 35-mm collagen-coated culture dishes. After cell attachment, the medium was replaced with fresh medium containing predetermined net magnetite concentrations (0–200 pg/cell), and a magnet (diameter: 30 mm; height: 15 mm; magnetic induction: 4000 Gauss) was then placed under the dish. The cells were incubated for an additional 6 h to label HepG2-HSP cells magnetically. After magnetic labeling of cells with MCLs, culture dishes were placed inside a horizontal coil (inner diameter: 7 cm; length: 7 cm), and an AMF was created using a transistor inverter (Dai-ichi High Frequency, Tokyo, Japan) (12). The magnetic field frequency and intensity were 120 kHz and 30.6 kA/m (386 Oe), respectively. The AMF was applied for 30 or 60 min. The medium temperature during AMF application was measured by an optical fiber probe (FX-9020; Anritsu Meter, Tokyo, Japan). At 48 h after magnetic heating, HepG2-HSP cells were observed under the BZ-9000 fluorescence microscope, and the EGFP expression level was analyzed by flow cytometry (SH800 Cell Sorter). The percentage of viable cells was determined as follows: cell viability (%) = (the number of viable cells in the tested dish)/(the number of viable cells in the control dish without AMF exposure) × 100.

Magnetic heating of multilayered HepG2-HSP cell sheets with MCLs To construct multilayered HepG2-HSP cell sheets, 1×10^6 HepG2-HSP cells labeled with MCLs were seeded in a 35-mm glass-bottom dish (Asahi Techno Glass; coverslip diameter: 12 mm). A cylindrical neodymium magnet was then placed under the dish to provide a magnetic force vertical to the dish, and the cells were cultured for 1 day. We designated this procedure as magnetic force-based tissue engineering (Mag-TE) (22). Cell culture dishes were placed inside a horizontal coil, and an AMF was applied for 60 min using the transistor inverter. The medium temperature during AMF application was measured by the optical fiber probe. At 48 h after magnetic heating, green fluorescence emitted by HepG2-HSP cell sheets was observed under a confocal laser-scanning microscope (Fluoview FV10i; Olympus, Tokyo, Japan). The total number of cell nuclei in cell sheets was counted using a NucleoCassette and NucleoCounte (Chemometec, Allerød, Denmark). The percentage of viable cells was determined as follows: cell viability (%) = (the number of cell nuclei in the tested sample)/(the number of cell nuclei in the non-heated control sample) × 100. For histological evaluation, HepG2-HSP cell sheets were washed three times with phosphate buffered saline (PBS), fixed in a 10% formaldehyde solution, and embedded in paraffin. Thin slices (4 μm) were prepared, stained with hematoxylin-eosin (H&E), and observed under the BZ-9000 microscope.

Plasmid construction for ferritin and DMT1 expression A DNA fragment encoding a fusion protein of human ferritin light chain-linker-human ferritin

heavy chain (17) was chemically synthesized (Eurofin, Tokyo, Japan) and ligated into pQMSCV/CMV/IRES/EGFP (23) to generate pQMSCV/CMV/Ferritin/IRES/EGFP. The EGFP region of pQMSCV/CMV/Ferritin/IRES/EGFP was replaced with the DNA fragment encoding mCherry (Takara Bio) by digestion with *Bst*XI and *Cla*I to generate pQMSCV/CMV/Ferritin/IRES/mCherry. To construct pCMV/DMT1/IRES/DsRed, a DMT1 cDNA fragment (Cat. No. MHS6278-202809112; Open Biosystems, Huntsville, AL, USA) was ligated into *Nhe*I and *Xho*I-digested pIRES2/DsRed/Express (Clontech Laboratories, Mountain View, CA, USA).

Magnetic cell labeling with ferritin Cells (2×10^6) were seeded in a 100-mm tissue culture dish (Greiner Bio-One). The next day, the cells were transfected with 24 μg DNA (pQMSCV/CMV/Ferritin/IRES/EGFP with/without pCMV/DMT1/IRES/DsRed for HeLa cells or pQMSCV/CMV/Ferritin/IRES/mCherry for HepG2-HSP cells) using Lipofectamine 2000. To load cells with Fe^{2+}, cells were transfected with pQMSCV/CMV/Ferritin/IRES/EGFP and pCMV/DMT1/IRES/DsRed. The transfection efficiency was approximately 30%. At 24 h post-transfection, the cells were incubated for 6 h in iron incorporation buffer [20 mM HEPES, 130 mM NaCl, 10 mM KCl, 1 mM $CaCl_2$, 1 mM $MgSO_4$ and 0.1 mM nifedipine (Wako Pure Chemical Industries, Osaka, Japan), pH 6.5] (18) containing 3 mM ferrous ammonium sulfate (Wako Pure Chemical Industries), 5% FBS, and 50 μM L-ascorbate (Sigma–Aldrich). To load cells with Fe^{3+}, cells were transfected with pQMSCV/CMV/Ferritin/IRES/EGFP. At 24 h post-transfection, the cells were incubated with culture medium containing 3 mM ferric ammonium citrate (Sigma–Aldrich) and 3 mM holo-transferrin (BBI Solutions, Cardiff, UK). Liposomal Fe^{2+} was prepared using ferrous ammonium sulfate (Wako Pure Chemical Industries) and a lipid mixture of TMAG (Sogo Pharmaceutical), DLPC (NOF), and DOPE (NOF) at a 1:2:2 molar ratio. The lipid mixture dissolved in chloroform was dried by evaporation for a minimum of 30 min. Lipids were hydrated by vortexing in a ferrous ammonium sulfate/PBS solution, and liposomes were sonicated for 60 min. To load cells with liposomal Fe^{2+}, cells were transfected with pQMSCV/CMV/Ferritin/IRES/EGFP for HeLa cells or pQMSCV/CMV/Ferritin/IRES/mCherry for HepG2-HSP cells. At 24 h post-transfection, the cells were incubated with culture medium containing liposomal Fe^{2+} (concentration of ferrous ammonium sulfate: 3 mM).

To measure the iron concentration and number of viable cells, iron-loaded cells were sampled and assayed by a method based on colorimetric quantification using potassium thiocyanate (24) and trypan blue dye exclusion, respectively. Briefly, after counting cells, cells were dissolved in 12N HCl solution, and then the solution was mixed with an equal volume of 5% trichloroacetic acid. After centrifugation for 10 min, the iron concentration in the supernatant was measured by the potassium thiocyanate method. The percentage of viable cells at 24 h after iron addition was determined as follows: cell viability (%) = (the number of viable cells in the tested dish)/(the number of viable cells in the untreated control dish) × 100.

MRI relaxometry HeLa cells magnetically labeled with ferritin were prepared as described above. At 48 h post-transfection, the cells were transferred to microcentrifuge tubes (4×10^6 cells/tube), centrifuged for 5 min at 200 ×*g*, and fixed in 4% paraformaldehyde. Supernatants were aspirated, and cell pellets were subjected to transverse (T_2) relaxation time measurements using a 1.5 T MRI (MRmini SA; DS Pharma Biomedical, Osaka, Japan). T_2 measurements were acquired using a multi-echo sequence with a repetition time TR of 2000 ms, inter-echo times of 69, 89, and 109 ms, 256 × 256 image points, and 15 (1-mm thick) slices through the cell pellets. A T_2 map was reconstructed from variable TE images using ImageJ (NMR imager). R_2 ($1/T_2$) values were calculated from the T_2 map in equivalent regions of each sample.

Magnetic cell separation At 24 h after iron loading, HeLa cells magnetically labeled with ferritin were subjected to a MACS magnetic cell separation system (Miltenyi Biotec, Bergisch Gladbach, Germany). Cells (1×10^7) were suspended in 0.5 mL MACS buffer (Miltenyi Biotec) and loaded onto an LS column (Miltenyi Biotec) that was equilibrated with MACS buffer. The column was washed three times with 1 mL MACS buffer, and the flow through population was collected. Cells captured in the magnetic field were eluted after removal of the magnet using 5 mL MACS buffer. Viable cells were counted using the trypan blue dye exclusion method, and the percentage of separated cells was determined as follows: separation (%) = (cell count of elute)/(total cell count) × 100.

Magnetic heating of cells magnetically labeled with ferritin At 24 h after iron loading, cells magnetically labeled with ferritin were transferred to microcentrifuge tubes (1×10^7 cells/tube) and centrifuged for 5 min at 1000 rpm. The tubes were placed inside the horizontal coil, and an AMF was applied with the transistor inverter as described above. For HeLa cells, the temperature in cell pellets was measured by the optical fiber probe, and the initial heating rate (0–2 min) was calculated. For HepG2-HSP cells, cells in the pellet were reseeded in a 6-well plate at 1×10^6 cells/well, and EGFP expression was analyzed under the fluorescence microscope and by flow cytometry at 48 h after magnetic heating.

Using HepG2-HSP cells (1×10^6) magnetically labeled with ferritin, cell sheets were constructed by the Mag-TE method, and an AMF was applied for 60 min using the transistor inverter as described above. At 48 h after magnetic heating, cell sheets were stained with 4′,6-diamidino-2-phenylindole (DAPI), and blue (DAPI) and green (EGFP) fluorescence emitted by HepG2-HSP cell sheets was observed under the confocal laser-scanning microscope.

Statistical analysis The Mann–Whitney rank sum test was used to evaluate the statistical significance of differences. Statistically significant differences were recognized at a *P*-value of less than 0.05.

RESULTS

Transgene expression profile of HepG2-HSP cells upon heating The gene circuit of the heat-inducible transgene expression system (Fig. S1) was transduced into HepG2 cells using a retroviral vector to establish HepG2-HSP cells as a heat-responsive designer cell line. To test heat inducibility, HepG2-HSP cells were heated in a WB (Fig. 1). Fig. 1A shows the gene expression profiles of HepG2-HSP cells heated at 39°C, 41°C, or 43°C for 60 min. Without heating, HepG2-HSP cells showed a negligible level of EGFP expression, indicating that the gene expression system in HepG2-HSP cells maintained a low basal expression level from the HSP70B' promoter. No significant expression of EGFP was observed in HepG2-HSP cells at 39°C, whereas EGFP expression was observed at 41°C, suggesting that the activation temperature of the HSP70B' promoter in HepG2-HSP cells was approximately 41°C. In flow cytometry, EGFP-positive cells were 14.9% and 41.7% of the total cell population at 41°C and 43°C, respectively (Fig. 1B). Heat treatment at 39°C or 41°C for 60 min did not affect cell viability, whereas a significant decrease in cell viability was observed when cells were heated at 43°C for 60 min (Fig. 1C). Interestingly, although we adopted a hybrid promoter consisting of $P_{HSP70B'}$ and TRE/$P_{CMVmini}$ for the heat-inducible expression system (Fig. S1), flow cytometry did not show a single EGFP-positive population of HepG2-HSP cells at 43°C (Fig. 1A), indicating that there were various populations of cells expressing different levels of the EGFP gene. To further analyze the transgene expression profile, EGFP-positive cells heated at 43°C for 60 min were sorted using a cell sorter. When the sorted cells were heated again in the WB at 41°C or 43°C for 60 min, two EGFP-positive cell populations clearly appeared in flow cytometry (Fig. 1C). Because the Tet-transactivator system was included in the heat-inducible gene expression system with the positive feedback loop for transcriptional gene amplification (Fig. S1), it was possible to cancel the effect of the Tet-mediated positive feedback loop for gene expression by Dox addition. The addition of Dox to cells heated at 41°C or 43°C for 60 min resulted in a single EGFP-positive cell population with a decreased intensity of green fluorescence (Fig. 1D), indicating that the enhancement in EGFP gene expression after heat treatment was caused by the positive feedback loop.

Magnetically triggered transgene expression of HepG2-HSP cells in monolayer culture For magnetic labeling of HepG2-HSP cells, MCLs were added to the medium in cell culture and a magnet was placed under the culture dish. A monolayer of HepG2-HSP cells was evenly labeled with MCLs (Fig. S2A). The amount of magnetite uptake was proportional to the concentration of MCLs added at 50–200 pg/cell, and 50%–75% of the added MCLs were taken up by HepG2-HSP cells (Fig. S2B). Moreover, MCL addition in the range of 50–200 pg/cell did not affect cell viability (Fig. S2A).

For magnetic heating, monolayered HepG2-HSP cells labeled with MCLs (100 pg magnetite/cell) were exposed to an AMF for 60 min (Fig. 2A–C). Although no substantial increase of bulk temperature during AMF exposure (Fig. 2A) and no significant decrease of cell viability after AMF exposure (Fig. 2B) were observed in the monolayered HepG2-HSP cell culture, EGFP expression was

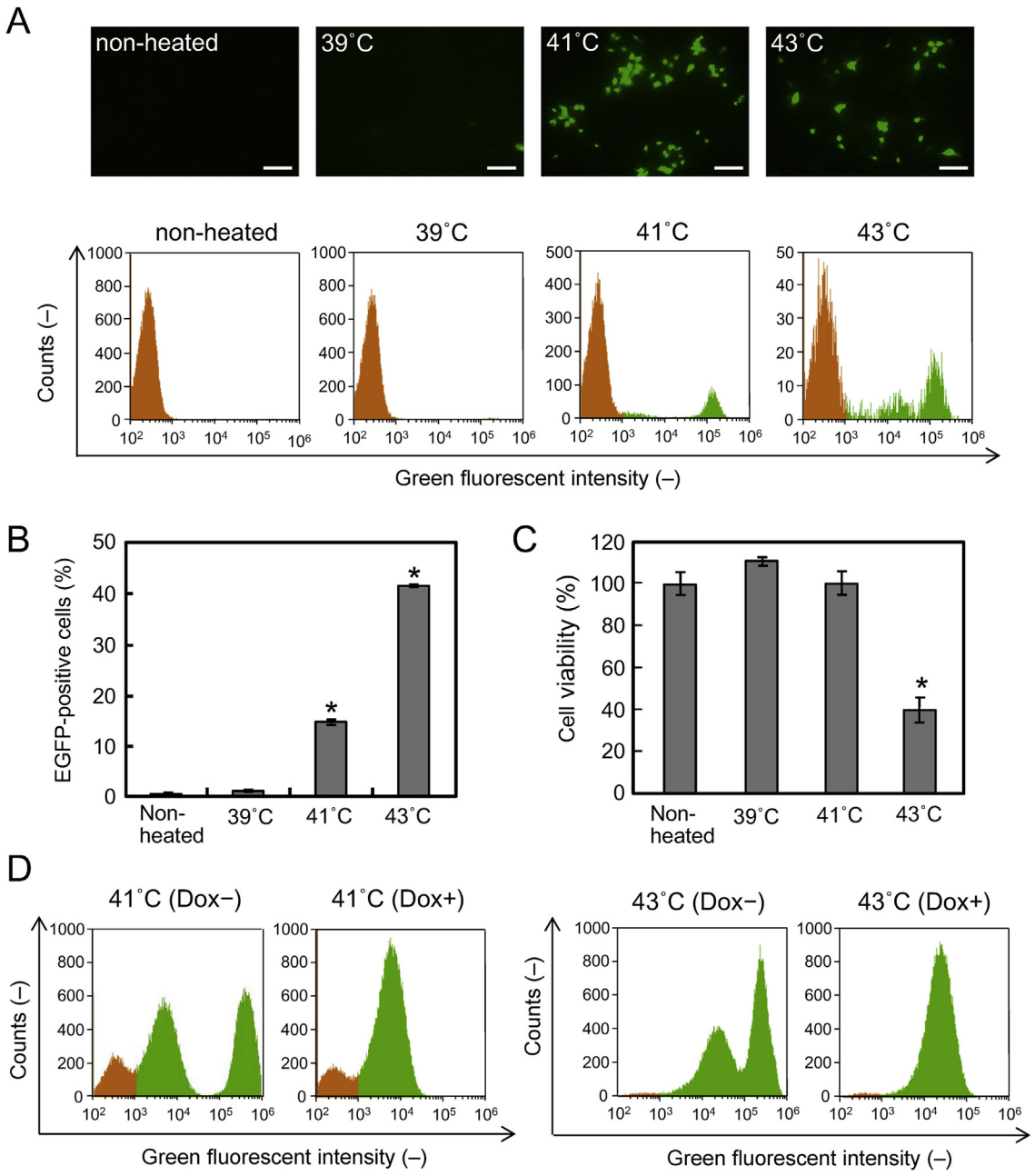

FIG. 1. Heat-induced transgene expression profile of HepG2-HSP cells. (A–C) HepG2-HSP cells were incubated at 37°C (non-heated) or heated in a water bath at 39°C, 41°C, or 43°C for 60 min. (A) Representative images of fluorescence microscopy (upper) and flow cytometry (bottom). Scale bars: 100 μm. In flow cytometry, EGFP-negative cell populations gated using non-heated cells are shown in orange, and EGFP-positive cell populations are shown in green. (B) Quantitative analysis of EGFP-positive cells by flow cytometry. Data are expressed as the mean ± SD of triplicates. *$P < 0.05$ vs. non-heated group. (C) Cell viability based on the trypan blue dye exclusion method. Data are expressed as the mean ± SD of triplicates. *$P < 0.05$ vs. non-heated group. (D) EGFP-positive cells heated at 43°C for 60 min (A) were sorted by a cell sorter. The sorted cells were cultured in medium containing doxycycline for 1 week to turn off EGFP gene expression due to the Tet-responsive system. The cells were then cultured without doxycycline for 3 days and then heated again in the water bath at 41°C or 43°C for 60 min in the presence (Dox+) or absence (Dox−) of doxycycline. EGFP-negative cell populations gated using non-heated cells are shown in orange, and EGFP-positive cell populations are shown in green.

observed at 48 h after AMF exposure (Fig. 2C). Fig. 2D shows the percentage of EGFP-positive HepG2-HSP cells in flow cytometry. HepG2-HSP cells showed a significantly high percentage of EGFP-positive cells when treated with MCLs at 25 pg/cell and the AMF for 30 min, and the percentage of EGFP-positive cells reached a maximum of approximately 20% when HepG2-HSP cells were treated with an MCL concentration of 50 pg/cell and AMF for 60 min. These results indicated that the genetically engineered cells labeled with magnetite nanoparticles successfully expressed the transgene through localized cellular heating by AMF exposure in monolayered cells without bulk heating in the culture medium.

Magnetically triggered transgene expression of HepG2-HSP cells with MCLs in multilayered cell sheets HepG2-HSP cells labeled with MCLs (magnetite addition: 100 pg/cell) were accumulated and stratified by magnetic force, and a multilayered sheet-like structure was formed at 1 day after the start of the 3D cell culture with a magnet (Fig. 3A). Histological analysis by H&E staining revealed that 3D cell sheets were approximately 30 μm in thickness and consisted of four cell layers (Fig. 3B). When HepG2-HSP cell sheets were exposed to the AMF for 60 min, no detectable increase of bulk temperature was observed in the culture medium (Fig. 3C). Additionally, no significant decrease of

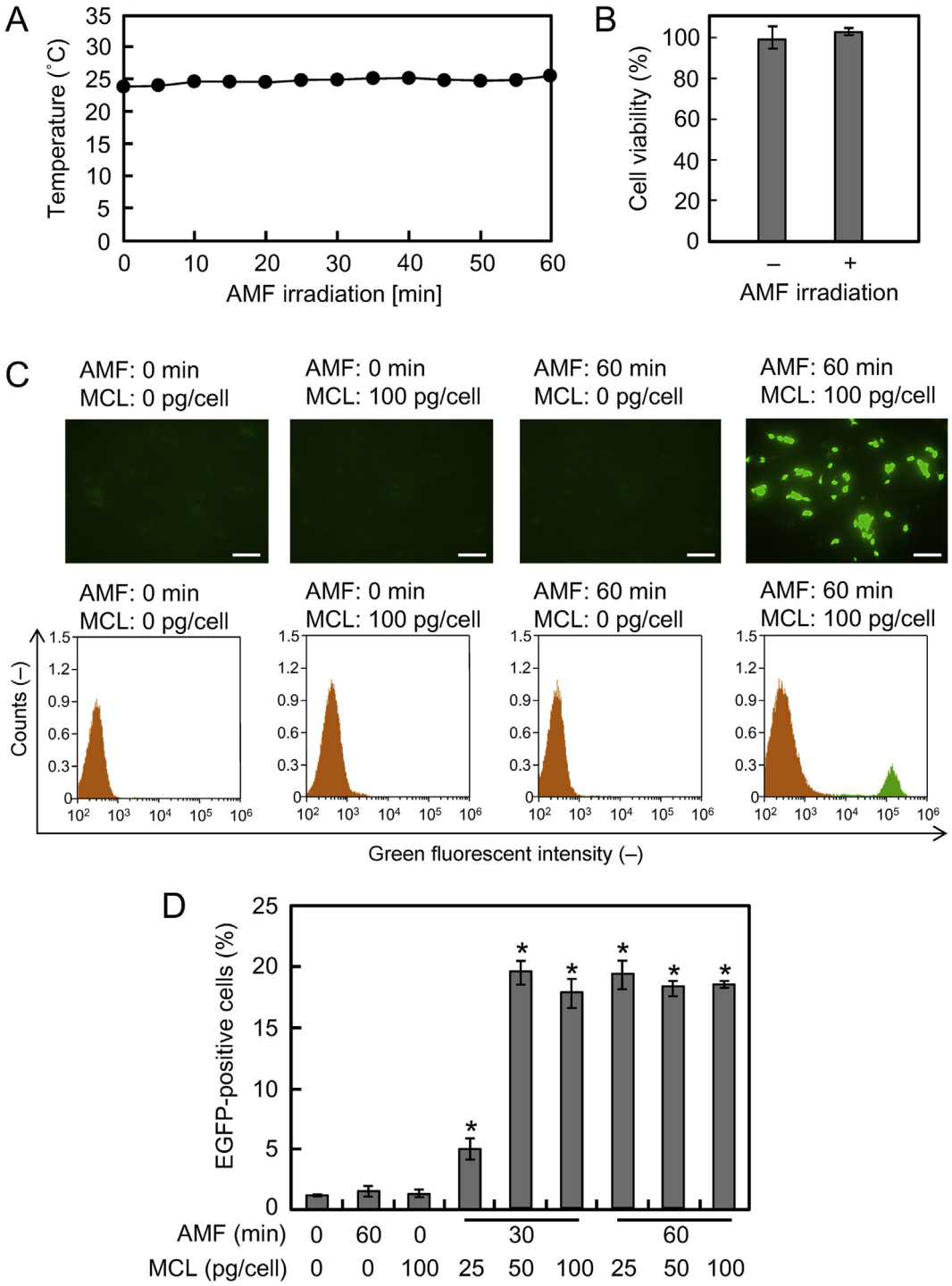

FIG. 2. Magnetically triggered EGFP gene expression in monolayered HepG2-HSP cells. (A–C) HepG2-HSP cells labeled with MCLs (100 pg magnetite/cell) in monolayer culture were exposed to an alternating magnetic field (AMF) for 60 min. (A) Time course of temperature in the culture medium during AMF exposure. (B) Cell viability based on the trypan blue dye exclusion method at 48 h after AMF exposure. Cells were treated with (+) or without (–) AMF. Data are expressed as the mean ± SD of triplicates. (C) Representative images of fluorescence microscopy (upper) and flow cytometry (bottom). Scale bars: 100 μm. In flow cytometry, EGFP-negative cell populations gated using control cells (AMF, 0 min; MCL, 0 pg/cell) are shown in orange, and EGFP-positive cell populations are shown in green. (D) Quantitative analysis of EGFP-positive cells in flow cytometry. Data are expressed as the mean ± SD of triplicates. $^*P < 0.05$ vs. control group (AMF, 0 min; MCL, 0 pg/cell).

cell viability was observed within the cell sheets (Fig. 3D). In contrast, EGFP expression of cell sheets was observed by confocal laser microscopy at 48 h after AMF exposure (Fig. 3E). Taken together, these results indicated that the genetically engineered cell sheets constructed by Mag-TE expressed the transgene through magnetic heating without cytotoxicity.

Magnetic cell labeling with ferritin We further investigated whether magnetic cells could be generated by a genetic engineering approach by ferritin gene transfer. First, we explored how to load cells with iron and tested three approaches (Fig. 4A). As shown in Fig. 4B, ferritin gene transfer into HeLa cells increased iron loading of both Fe^{2+} and Fe^{3+}, and DMT1 gene transfection and

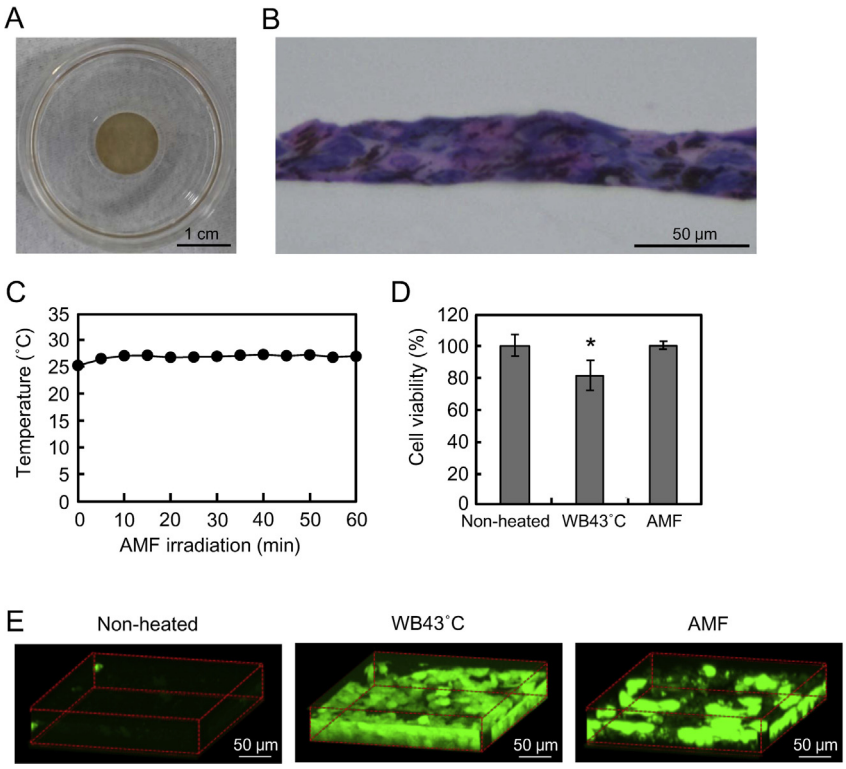

FIG. 3. Magnetically triggered EGFP gene expression in multilayered HepG2-HSP cell sheets. (A) Macroscopic image of a cell sheet. HepG2-HSP cells were labeled with MCLs (100 pg magnetite/cell), and cell sheets were constructed by a Mag-TE technique. Cell sheets had a black-brown color because of magnetite nanoparticles. (B) Representative bright field micrograph of a hematoxylin/eosin-stained cross-section of a cell sheet. (C) Time course of temperature in the culture medium during AMF exposure. (D and E) HepG2-HSP cell sheets were incubated at 37°C (non-heated) or heated in a water bath at 43°C for 60 min (WB43°C) or exposure to an AMF for 60 min (AMF). (D) Cell viability based on counting the total number of cell nuclei in cell sheets at 48 h after AMF exposure. Data are expressed as the mean ± SD of triplicates. $^*P < 0.05$ vs. non-heated group. (E) Representative fluorescence microscopy images of cell sheets.

transferrin addition augmented the cellular iron levels of Fe^{2+} and Fe^{3+}, respectively. A similar level of cellular iron (2.5 pg/cell) was also achieved by addition of liposomal Fe^{2+}. Fig. 4C shows cell viability after iron loading: Addition of Fe^{2+} resulted in low cell viability compared with Fe^{3+}, whereas liposomal Fe^{2+} loading led to a relatively higher level of cell viability compared with Fe^{2+} plus DMT1 gene transfection or Fe^{3+} plus transferrin addition.

Magnetic property of the ferritin-engineered cells To confirm the magnetic behavior of cells producing iron-loaded ferritin, we investigated MRI, magnetic separation, and magnetic heating of the ferritin-engineered cells. The NMR transverse relaxation rates (R_2) of HeLa cell pellets magnetically labeled with ferritin are shown in Fig. 5A. Overall, the ferritin-engineered cell pellets showed a significantly higher R_2 relaxation rate compared with untreated cell pellets. In addition, as expected, the results of T_2-weighted MRI showed that the ferritin-engineered cell pellets were darker than untreated cell pellets.

To investigate whether the ferritin-engineered cells could be separated magnetically, cells were applied to a commercially available MACS column and allowed to separate in the presence of a magnetic field produced by the MACS device. Fig. 5B shows that ferritin-engineered HeLa cells were separated at a rate of 20%–30%.

Next, we examined magnetic heating of ferritin-engineered HeLa cells using liposomal Fe^{2+}. Liposomal Fe^{2+} was used because liposomal Fe^{2+} showed the highest cellular iron concentration (Fig. 4B) with less toxicity (Fig. 4C). As shown in Fig. 5C, the initial heating rate of ferritin-engineered HeLa cell pellets exposed to an AMF was slightly but not significantly higher than that of untreated cells. We next conducted magnetic cell separation. The heating rate of cell pellets derived from magnetically captured cells was significantly higher than that of untreated cells or flow through cells, indicating that the ferritin-engineered cells generated heat under AMF application.

Magnetically triggered transgene expression of ferritin-engineered HepG2-HSP cells When a pellet of ferritin-engineered HepG2-HSP cells was exposed to an AMF for 60 min, induced expression of EGFP was observed in approximately 5% of total cells (Fig. 6A–C), and the expression level was decreased by Dox addition, indicating that the high level expression of EGFP was caused by the positive feedback system. Moreover, the ferritin-engineered HepG2-HSP cells formed a multilayered sheet-like structure, and EGFP expression was observed by confocal laser microscopy at 48 h after AMF exposure (Fig. 6D). Taken together, these results indicate that magnetic cells can be generated by overexpressing the ferritin gene without the addition of inorganic magnetic nanoparticles, and AMF exposure induces transgene expression in ferritin-engineered cells.

DISCUSSION

Recently, remote control of transgene expression through a magnetic field has attracted attention in bioscience and biomedical fields. Huang et al. (25) showed that magnetic heating of 6 nm manganese ferrite ($MnFe_2O_4$) by an AMF (40 MHz) remotely activates the temperature-sensitive calcium ion channel TRPV1 in neuronal cells. The heat generation of magnetic nanoparticles during AMF exposure is proportional to the frequency (Hz), whereas a frequency above 1 MHz generates non-specific heating of the surrounding tissues because of eddy currents and/or dielectric loss (26). In our preclinical studies of MFH for cancer, a

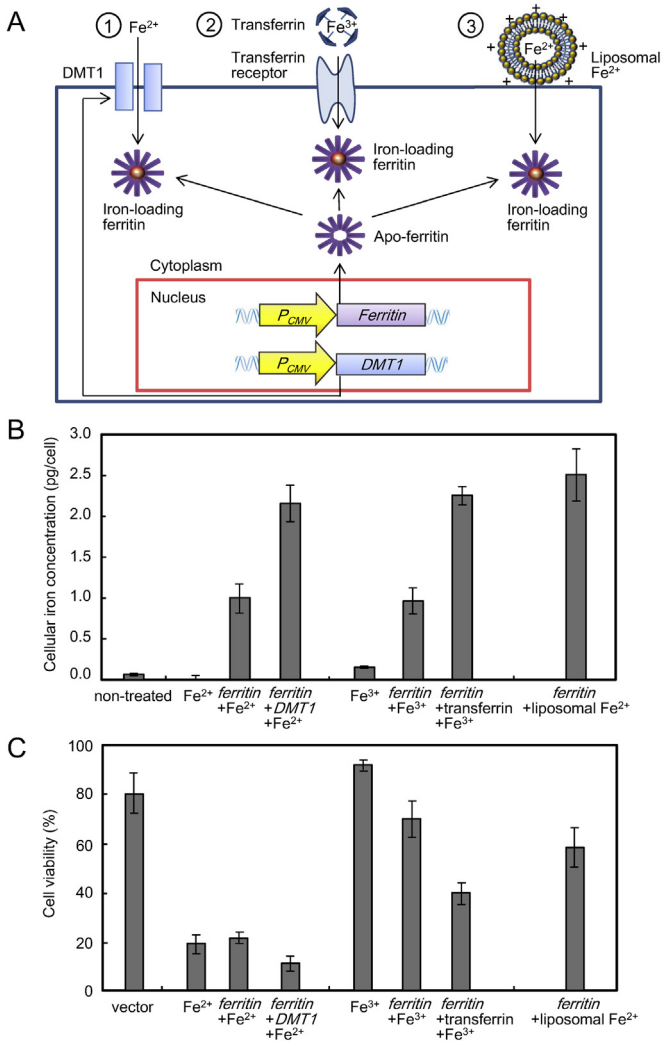

FIG. 4. Magnetic labeling of HeLa cells with ferritin. (A) Diagram showing three strategies for loading ferritin-engineered cells with iron. HeLa cells are transfected with the ferritin gene driven by the constitutive cytomegalovirus promoter P_{CMV}, and expression of the ferritin gene leads to production of apoferritin: 1, To load cells with Fe^{2+}, the cells are co-transfected with the DMT-1 gene driven by the CMV promoter, and plasma membrane-bound DMT-1 acts as an importer for Fe^{2+} of ferrous ammonium sulfate added to the culture medium. 2, To load cells with Fe^{3+}, the cells are treated with transferrin by incubating with culture medium containing ferric ammonium citrate and holo-transferrin. Transferrin binds to the transferrin receptor, and Fe^{2+} is endocytosed. 3, Cationic liposomes are taken up by cells, and Fe^{2+} is endocytosed. These intracellular irons are supplied for iron-loading of ferritin. (B) Cellular iron concentration in HeLa cells at 24 h after iron addition. Non-treated: cells without both transfection and iron addition. Data are expressed as the mean ± SD of triplicates. (C) Cell viability based on the trypan blue dye exclusion method at 24 h after iron addition. Vector: mock transfection control to assess the effect of the transfection reagent on the cells. Data are expressed as the mean ± SD of triplicates.

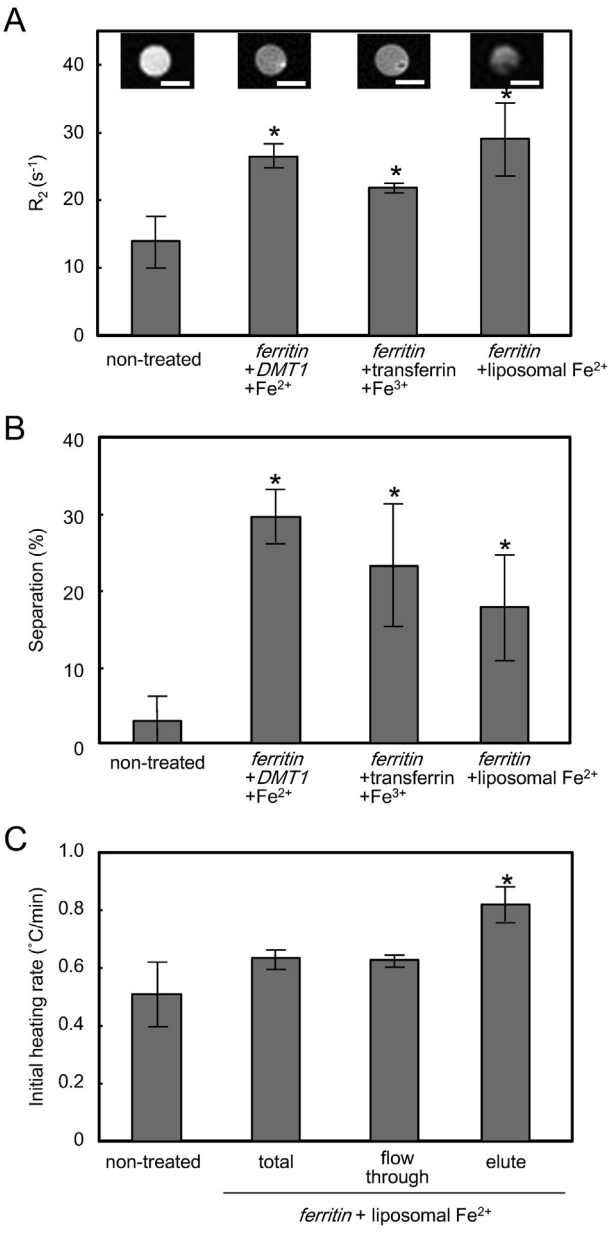

FIG. 5. Magnetic property of ferritin-engineered HeLa cells. (A) NMR relaxation rates and MRI (inset; scale bars: 2 mm) of ferritin-engineered cell pellets at 24 h after iron loading. Data are expressed as the mean ± SD of triplicates. $^*P < 0.05$ vs. non-treated group. (B) Magnetic separation of ferritin-engineered cells at 24 h after iron loading. Data are expressed as the mean ± SD of triplicates. $^*P < 0.05$ vs. non-treated group. (C) Magnetic heating of ferritin-engineered cells. HeLa cells were transfected with the ferritin gene and loaded with liposomal Fe^{2+}. At 24 h after iron loading, ferritin-engineered cells were pelleted (total). Moreover, ferritin-engineered cells were magnetically separated by the MACS system, and the flow through or magnetically captured (elute) cells were also pelleted. These cell pellets were exposed to an AMF, and initial heating rates were calculated. Data are expressed as the mean ± SD of triplicates. $^*P < 0.05$ vs. non-treated group.

magnetic field with a frequency of 120 kHz was chosen as the optimal frequency without generating non-specific heating. Thus, we adopted 120 kHz in the present study. In terms of magnetic nanoparticles, the heating capacity correlates with the particle size, which is evidence that the mechanism of heat generation is Néel relaxation. For medical application, magnetic particles are required to be well dispersed in water, and, in our experience, the particle size should be less than 15 nm. Furthermore, the lack of intrinsic cytotoxicity is the most obvious criterion, especially for medical application, and Fe_3O_4 and Fe_2O_3 nanoparticles have been used because of their biocompatibility. In the present study, we used 10 nm Fe_3O_4 magnetite nanoparticles and a 120 kHz AMF generator.

We previously reported that MCL uptake by HepG2 cells is 48.9 pg/cell at 24 h after addition of MCLs (100 pg/cell) (27). In the present study, we placed a magnet under the culture dish to attract MCLs onto monolayered cells to enhance the amount of magnetite uptake. As a result, MCL uptake by HepG2 cells was enhanced to 75.2 pg/cell at 6 h after addition of MCLs (100 pg magnetite/cell) (Fig. S2B), suggesting that magnetic attraction of MCLs improves their uptake by target cells. In this study, we used human hepatoma HepG2 cells as a model for designer mammalian cells. Because the

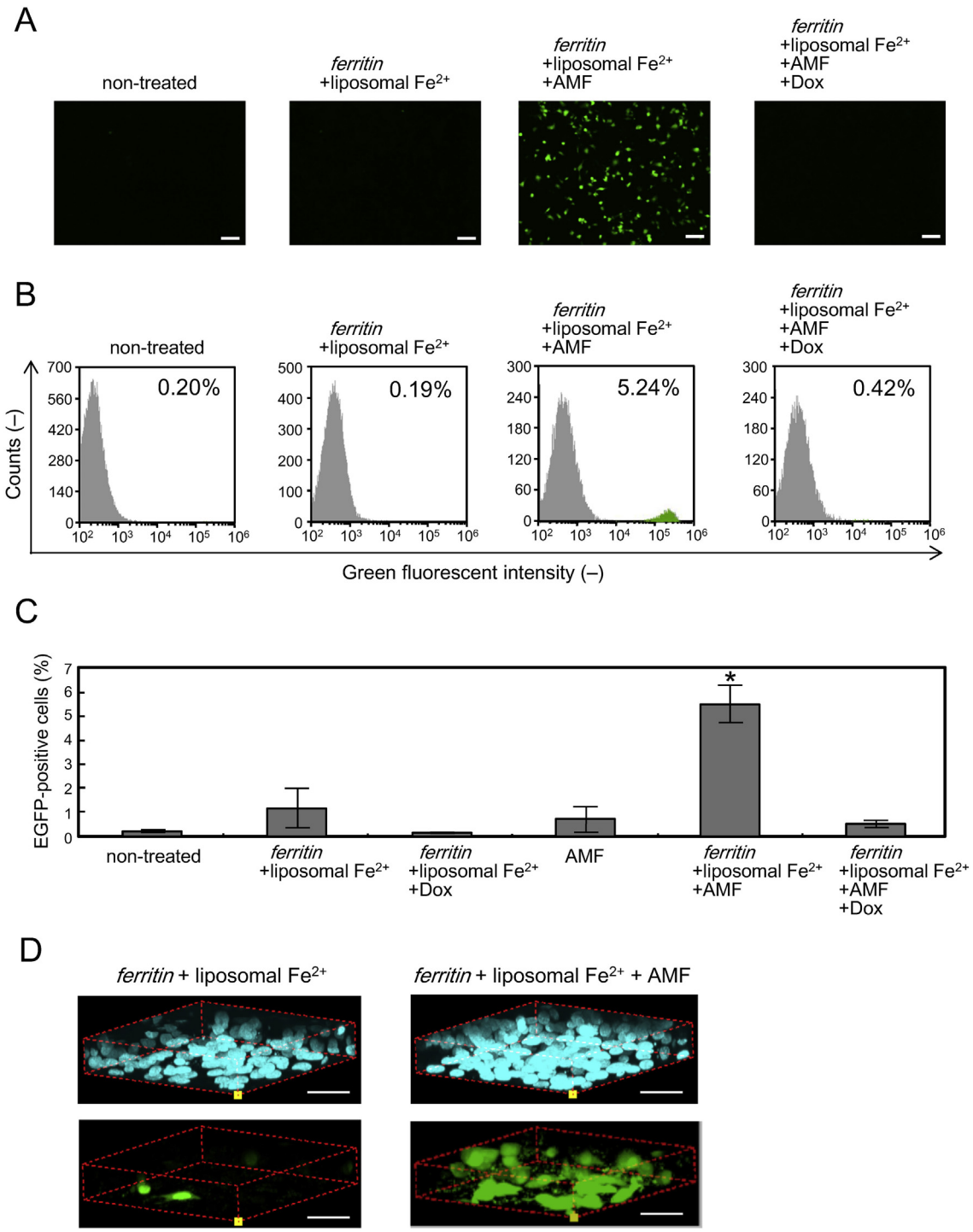

FIG. 6. Magnetic heating of HepG2-HSP cells magnetically labeled with ferritin. (A–C) Magnetic heating of ferritin-engineered HepG2-HSP cell pellets. At 24 h after iron loading, cells magnetically labeled with ferritin were pelleted and exposed to an AMF for 60 min. Cells in the pellets were reseeded, and EGFP expression was observed under a fluorescence microscope (Scale bars: 200 μm) (A) or analyzed by flow cytometry (B) at 48 h after magnetic heating. EGFP-positive cells were also quantified by flow cytometry (C). Data are expressed as the mean ± SD of triplicates. $^*P < 0.05$ vs. non-treated group. (D) Cell sheets of ferritin-engineered HepG2-HSP cells were constructed by the magnetic force-based tissue engineering method, and an AMF was applied for 60 min. At 48 h after magnetic heating, cell sheets were stained with DAPI, and blue and green fluorescence in HepG2-HSP cell sheets were observed using a confocal laser-scanning microscope. Scale bars: 50 μm.

degree of MCL uptake differs among cell types (27), uptake and cytotoxicity of MCLs in target cells should be tested before clinical application.

Using a synthetic biological approach, Stanley et al. (28) reported engineered insulin gene expression driven by magnetic heating of 20 nm magnetite nanoparticles through AMF exposure (465 kHz). TRPV1 was heated by AMF exposure, which allowed TRPV1 to gate calcium ions, leading to stimulated gene expression of engineered insulin driven by a calcium ion-sensitive synthetic promoter. The activation temperature of the TRPV1 protein is 42°C (29). In the present study, we used the HSP70B' promoter, and the temperature profile showed that the activation temperature of the HSP70B' promoter cells was 41°C (Fig. 1), which is relatively close to normal body temperature. In a previous study (30), we showed that

the expression level of a target gene driven by the HSP70B' promoter increases as heating temperature increases within the range of 37–45°C. However, heating at 43°C in a WB reduced cell viability (Fig. 1C). Unlike hyperthermia heating above 43°C to destroy tumor tissues, the designer cells in cell therapy including regenerative medicine should not be killed by heating. In the present study, the positive feedback loop in the heat-inducible transgene expression system (Fig. S1) enabled us to augment expression levels of the transgene even at the mild temperature of 41°C (Fig. 1). In the heat-inducible transgene expression system, we adopted the hybrid promoter system consisting of $P_{HSP70B'}$ and TRE/P_{CMVmin} (Fig. S1). Nevertheless, two populations of HepG2-HSP cells expressing high (with the positive feedback loop) and low (without the positive feedback loop) levels of EGFP were observed after heat treatment (Fig. 1D). The mechanism by which the heat-inducible transgene expression system caused two heat-induced expression patterns remains to be elucidated. A possible mechanism is that the two promoters, $P_{HSP70B'}$ and TRE/P_{CMVmin}, were located closely to each other, and each promoter interrupted the others transcriptional activity. As a solution, this promoter interference might be overcome by dividing the one-pack gene expression cassette used in the present study into two gene expression units in which each incorporates $P_{HSP70B'}$ or TRE/P_{CMVmin}.

In the present study, the percentage of EGFP-positive cells after magnetic heating was a maximum of approximately 20% (Fig. 2D), which was lower than that after WB heating at 43°C as a positive control (41.7%) (Fig. 1B). As discussed in a theoretical study reported by Rabin (31), an increase in bulk temperature surrounding a single cell (e.g., in monolayered cell culture) by magnetic heating is considered difficult to achieve, and the conditions of MFH (>43°C) can be met within a cluster/aggregate of magnetically labeled cells. Recent progress in nano-thermometers has begun to overcome the difficulty to measure the temperature of magnetic nanoparticles in single cells. Using synthesized fluorophores as a nano-thermometer, Huang et al. (25) measured the temperature distribution around nanoparticles in cells, and demonstrated that the surface of nanoparticles was heated significantly above the ambient temperature. In the present study, magnetic heating of nanoparticles in HepG2-HSP cells caused no appreciable bulk heating in the monolayered cell culture (Fig. 2A), but transgene expression was driven by the HSP70B' promoter (Fig. 2D). These results suggest that localized cellular heating of magnetite nanoparticles successfully activated the HSP70B' promoter as a switch, which in turn activated the positive feedback loop as an amplifier to enhance the expression level of the transgene by magnetic heating in the monolayered cell culture.

A major limitation of tissue-engineered constructs is the lack of nutrient and/or oxygen supply due to deficient vascularization (32). In scaffold-free cell sheets, multilayered cell culture at a high cell density is often limited by oxygen diffusion, and the thickness limitation to prevent ischemia in transplantation is 50–100 μm (33). In the present study, four cell-layered cell sheets of 30 μm in thickness were constructed by Mag-TE using 1×10^6 cells (Fig. 3B) that corresponds to approximately 4-fold of the confluent concentration against the culture area. Rabin reported that magnetic heating is sufficient to create necessary conditions for MFH (>43°C) only in a cluster of several cells fully loaded with magnetic nanoparticles and an overall diameter of at least 1 mm (31). Compared with monolayered cell culture, multilayered cell sheets can be easily heated by magnetic heating. However, in the present study, no significant increase in bulk temperature was detected in the culture medium of cell sheets (Fig. 3C) with a thickness of 30 μm (Fig. 3B), and no significant decrease of cell viability was observed in cell sheets (Fig. 3D). These results suggest that the temperature around cell sheets decreased rapidly, causing no observable bulk heating in the culture medium. Moreover, transgene expression of magnetically labeled HepG2-HSP cells in cell sheets was successfully induced through localized cellular heating by AMF exposure (Fig. 3E) without cytotoxicity. These results suggest the feasibility of magnetically triggered gene therapy using designer cell sheets constructed by Mag-TE.

Intracellular magnetic nanoparticle synthesis based on ferritin gene transfer into target cells is an attractive idea, especially in the synthetic biology field. According to a theoretical estimation reported by Kim et al. (18), transgene expression driven by a strong promoter, such as the CMV promoter, in mammalian cells typically reaches ~2.5 pg/cell. In this case, ferritin expression is up to 0.5 pg/cell and the total number of ferritin proteins is 6.4×10^5 ferritins/cell. The intracellular iron concentration required to achieve a maximum iron load is 1.6 mM. Therefore, in the present study, we added iron at a concentration of 3 mM and achieved a cellular iron concentration of 2–2.5 pg/cell that is similar to the experimental data (2.9 pg/cell) reported by Kim et al. (18) as well as their theoretical consideration (1.3 pg/cell). Among the iron-loading strategies conducted in the present study (Fig. 4A), we found that liposomal Fe^{2+} was the most efficient (Fig. 4B,C), and we obtained a sufficient number of magnetically labeled target cells for experiments. Compared with Fe^{3+}, Fe^{2+} addition to culture medium may cause cytotoxic effects owing to the hydroxyl radical generated by the Fenton reaction. We speculate that encapsulating Fe^{2+} in liposomes reduces cytotoxicity caused by sedimentation of iron on the target cells during cell culture. On the other hand, uptake of Fe^{3+} may depend on the level of transferrin receptor expression in target cells. In the present study, to investigate the approaches to augment iron uptake by ferritin-engineered cells, we used HeLa cells as a model cell line. Although it may be necessary to optimize iron-loading conditions for target cells before practical applications, we propose that liposomal Fe^{2+} is a useful tool to augment iron uptake by ferritin-engineered cells.

In addition to externally added magnetic nanoparticles such as MCLs, intracellular ferritin nanoparticles may be used for medical applications. In the present study, the ferritin-engineered cells augmented the NMR relaxation rate R_2 for MRI by 1.5–2.0 times (Fig. 5A) and showed an efficiency of 20%–30% in magnetic separation (Fig. 5B), which are comparable to previous studies of MRI by Iordanova et al. (17) (1.7 times) and magnetic separation by Kim et al. (18) (25%), respectively. For magnetic heating, the initial heating rate showed a significantly higher level compared with the control, although the heating rate was low (Fig. 5C). Recently, Meister (34) indicated that the iron core (5–6 nm) of ferritin is not considered useful for magnetic hyperthermia, and the ferric hydroxide material in ferritin has lower magnetic susceptibility than magnetite (~8 times). However, we hypothesized that localized intracellular heating could trigger transgene expression driven by the HSP70B' promoter, and transgene expression was induced in ferritin-engineered HepG2-HSP cells by AMF exposure (Fig. 6), although the expression level was low. In the present study, a monolayer of the ferritin-engineered HepG2-HSP cells did not express EGFP under AMF exposure (data not shown), whereas transgene expression in cell pellets (Fig. 6A–C) and cell sheets (Fig. 6D) was induced by AMF exposure. These results suggest that multilayered cell sheets are advantageous for heat-induced transgene expression by localized cellular heating of magnetic nanoparticles under AMF exposure. Cell sheet engineering is a promising approach for regenerative medicine (35), and magnetic labeling using the ferritin gene is a possible approach for magnetically triggered gene therapy using cell sheets for regenerative medicine.

By combining nanotechnology and synthetic biology, we have demonstrated an approach using localized cellular heating of magnetic nanoparticles to convert a magnetic signal into cell stimulation for transgene expression. This approach may be applicable to not only biological research, but also to novel gene

therapies in cell-based medicine such as regenerative medicine, based on remote manipulation of cellular functions via transgene expression in a spatiotemporal manner.

Supplementary data to this article can be found online at https://doi.org/10.1016/j.jbiosc.2019.03.008.

ACKNOWLEDGMENTS

This work was supported in part by a Grant-in-Aid for Scientific Research on Innovative Areas (No. 16H01393) from the Ministry of Education, Culture, Sports, Science and Technology (MEXT) of Japan. We thank Mitchell Arico from Edanz Group for editing a draft of this manuscript. The authors have no other relevant affiliations of financial involvement with any organization or entity with a financial interest in or financial conflict with the subject matter or materials discussed in the manuscript apart from those disclosed.

References

1. **Ausländer, S. and Fussenegger, M.:** From gene switches to mammalian designer cells: present and future prospects, Trends Biotechnol., **31**, 155–168 (2013).
2. **Haellman, V. and Fussenegger, M.:** Synthetic biology -Toward therapeutic solutions, J. Mol. Biol., **428**, 945–962 (2016).
3. **Cotto, J. J., Kline, M., and Morimoto, R. I.:** Activation of heat shock factor 1 DNA binding precedes stress-induced serine phosphorylation. Evidence for a multistep pathway of regulation, J. Biol. Chem., **271**, 3355–3358 (1996).
4. **Leung, T. K., Rajendran, M. Y., Monfries, C., Hall, C., and Lim, L.:** The human heat-shock protein family. Expression of a novel heat-inducible HSP70 (HSP70B') and isolation of its cDNA and genomic DNA, Biochem. J., **267**, 125–132 (1990).
5. **Gossen, M. and Bujard, H.:** Tight control of gene expression in mammalian cells by tetracycline-responsive promoters, Proc. Natl. Acad. Sci. USA, **89**, 5547–5551 (1992).
6. **Yamaguchi, M., Ito, A., Okamoto, N., Kawabe, Y., and Kamihira, M.:** Heat-inducible transgene expression system incorporating a positive feedback loop of transcriptional amplification for hyperthermia-induced gene therapy, J. Biosci. Bioeng., **114**, 460–465 (2012).
7. **Ito, A., Shinkai, M., Honda, H., and Kobayashi, T.:** Medical application of functionalized magnetic nanoparticles, J. Biosci. Bioeng., **100**, 1–11 (2005).
8. **Johannsen, M., Thiesen, B., Wust, P., and Jordan, A.:** Magnetic nanoparticle hyperthermia for prostate cancer, Int. J. Hyperthermia, **26**, 790–795 (2010).
9. **Ito, A., Yamaguchi, M., Okamoto, N., Sanematsu, Y., Kawabe, Y., Wakamatsu, K., Ito, S., Honda, H., Kobayashi, T., Nakayama, E., and other 5 authors:** T-cell receptor repertoires of tumor-infiltrating lymphocytes after hyperthermia using functionalized magnetite nanoparticles, Nanomedicine (Lond.), **8**, 891–902 (2013).
10. **Dennis, C. L. and Ivkov, R.:** Physics of heat generation using magnetic nanoparticles for hyperthermia, Int. J. Hyperthermia, **29**, 715–729 (2013).
11. **Hergt, R., Dutz, S., and Röder, M.:** Effects of size distribution on hysteresis losses of magnetic nanoparticles for hyperthermia, J. Phys. Condens. Matter, **20**, 385214 (2008).
12. **Shinkai, M., Yanase, M., Honda, H., Wakabayashi, T., Yoshida, J., and Kobayashi, T.:** Intracellular hyperthermia for cancer using magnetite cationic liposomes: in vitro study, Jpn. J. Cancer Res., **87**, 1179–1183 (1996).
13. **Imai, T., Kikumori, T., Akiyama, M., Yokota, K., Nishida, Y., Fujimoto, Y., Yamamoto, N., and Furue, H.:** A phase I study of hyperthermia using magnetite cationic liposome and alternating magnetic field for various refractory malignancies, Thermal Med., **27**, 74 (2011) (in Japanese).
14. **Yamaguchi, M., Ito, A., Ono, A., Kawabe, Y., and Kamihira, M.:** Heat-inducible gene expression system by applying alternating magnetic field to magnetic nanoparticles, ACS Synth. Biol., **3**, 273–279 (2014).
15. **Bacchus, W. and Fussenegger, M.:** The use of light for engineered control and reprogramming of cellular functions, Curr. Opin. Biotechnol., **23**, 695–702 (2012).
16. **Theil, E. C.:** Ferritin: the protein nanocage and iron biomineral in health and in disease, Inorg. Chem., **52**, 12223–12233 (2013).
17. **Iordanova, B., Robison, C. S., and Ahrens, E. T.:** Design and characterization of a chimeric ferritin with enhanced iron loading and transverse NMR relaxation rate, J. Biol. Inorg. Chem., **15**, 957–965 (2010).
18. **Kim, T., Moore, D., and Fussenegger, M.:** Genetically programmed superparamagnetic behavior of mammalian cells, J. Biotechnol., **162**, 237–245 (2012).
19. **Kawabata, H.:** Transferrin and transferrin receptors update, Free Radic. Biol. Med., **133**, 46–54 (2019).
20. **Yamamoto, H., Kawabe, Y., Ito, A., and Kamihira, M.:** Enhanced liver functions in mouse hepatoma cells by induced overexpression of liver-enriched transcription factors, Biochem. Eng. J., **60**, 67–73 (2012).
21. **Hotta, A., Saito, Y., Kyogoku, K., Kawabe, Y., Nishijima, K., Kamihira, M., and Iijima, S.:** Characterization of transient expression system for retroviral vector production, J. Biosci. Bioeng., **101**, 361–368 (2006).
22. **Ito, A. and Kamihira, M.:** Tissue engineering using magnetite nanoparticles, Prog. Mol. Biol. Transl. Sci., **104**, 355–395 (2011).
23. **Ito, A., Takahashi, T., Kawabe, Y., and Kamihira, M.:** Human beta defensin-3 engineered keratinocyte sheets constructed by a magnetic force-based tissue engineering technique, J. Biosci. Bioeng., **108**, 244–247 (2009).
24. **Owen, C. S. and Sykes, N. L.:** Magnetic labeling and cell sorting, J. Immunol. Methods, **73**, 41–48 (1984).
25. **Huang, H., Delikanli, S., Zeng, H., Ferkey, D. M., and Pralle, A.:** Remote control of ion channels and neurons through magnetic-field heating of nanoparticles, Nat. Nanotechnol., **5**, 602–606 (2010).
26. **Hergt, R., Dutz, S., Müller, R., and Zeisberger, M.:** Magnetic particle hyperthermia: nanoparticle magnetism and materials development for cancer therapy, J. Phys. Condens. Matter, **18**, S2919–S2934 (2006).
27. **Ito, A., Jitsunobu, H., Kawabe, Y., and Kamihira, M.:** Construction of heterotypic cell sheets by magnetic force-based 3-D coculture of HepG2 and NIH3T3 cells, J. Biosci. Bioeng., **104**, 371–378 (2007).
28. **Stanley, S. A., Gagner, J. E., Damanpour, S., Yoshida, M., Dordick, J. S., and Friedman, J. M.:** Radio-wave heating of iron oxide nanoparticles can regulate plasma glucose in mice, Science, **336**, 604–648 (2012).
29. **Caterina, M. J., Schumacher, M. A., Tominaga, M., Rosen, T. A., Levine, J. D., and Julius, D.:** The capsaicin receptor: a heat-activated ion channel in the pain pathway, Nature, **389**, 816–824 (1997).
30. **Ito, A., Okamoto, N., Yamaguchi, M., Kawabe, Y., and Kamihira, M.:** Heat-inducible transgene expression with transcriptional amplification mediated by a transactivator, Int. J. Hyperthermia, **28**, 788–798 (2012).
31. **Rabin, Y.:** Is intracellular hyperthermia superior to extracellular hyperthermia in the thermal sense? Int. J. Hyperthermia, **18**, 194–202 (2002).
32. **Lovett, M., Lee, K., Edwards, A., and Kaplan, D. L.:** Vascularization strategies for tissue engineering, Tissue Eng. Part B Rev., **15**, 353–370 (2009).
33. **Matsuura, K., Utoh, R., Nagase, K., and Okano, T.:** Cell sheet approach for tissue engineering and regenerative medicine, J. Control. Release, **190**, 228–239 (2014).
34. **Meister, M.:** Physical limits to magnetogenetics, Elife, **5**, e17210 (2016).
35. **Nagase, K., Yamato, M., Kanazawa, H., and Okano, T.:** Poly(*N*-isopropylacrylamide)-based thermoresponsive surfaces provide new types of biomedical applications, Biomaterials, **153**, 27–48 (2018).